

## ***B* production in pPb at 5.02 TeV from CMS**

Kisoo Lee (for the CMS collaboration)<sup>1</sup>

<sup>1</sup>*Korea University, Seoul 136-701, Republic of Korea*

**Abstract.** Hadrons with heavy quarks are promising probes to investigate the detailed properties of hot and dense medium generated by heavy-ion collisions at collider energies. Since heavy quarks are sensitive to the transport properties of the medium, the energy-loss pattern of them is expected to be quite different from that of light quarks in a strongly-interacting matter. On the other hand, in order to elicit the actual effects caused by the hot and dense medium, it is necessary to understand the cold nuclear matter effect in pA collisions. For example, the pPb data is expected to provide a baseline for the study of the b-quark energy loss in medium produced by PbPb collisions. Therefore, the CMS Collaboration at the Large Hadron Collider (LHC) has analyzed the production cross sections of  $B^+$ ,  $B^0$ ,  $B_s^0$  mesons in pPb collisions as a function of rapidity and the transverse momentum at the nucleon-nucleon center-of-mass energy of 5.02 TeV. In addition, the nuclear modification factors of the  $B$  mesons have been constructed using the theoretical pp reference spectra estimated by the perturbative Quantum ChromoDynamics (pQCD) model. Finally CMS collected pp and PbPb collisions at the center-of-mass energy of 5.02 TeV at the LHC in the end of 2015. Analysis of  $B$  production in pp and PbPb is ongoing.

### **1 Introduction**

In the heavy-ion collisions, heavy quarks are useful probe to study hot and dense QCD medium because they are produced in the early stage of collision and interact with medium. Besides, there may be effects due to nuclear modifications to the parton distributions, known as the cold nuclear matter effect, such as nuclear modifications to the parton distributions. The pPb collisions are considered as a useful system to study the cold nuclear matter effect because they are not expected to form an extended hot medium. With large cross section of b quark production at the LHC, the CMS collaboration has measured production cross section of b quarks. The CMS collaboration studied the b-hadron production in PbPb collisions at  $\sqrt{s_{NN}} = 2.76$  TeV by using inclusive non-prompt  $J/\psi$  in the 2010 and 2011 data sets [1]. For the first time, CMS collaboration reconstructed exclusive  $B$  mesons via the combination of charged particle tracks to the reconstructed  $J/\psi$  in the pPb collisions at  $\sqrt{s_{NN}} = 5.02$  TeV recorded in 2013.

The  $B$  meson species analyzed for this study are  $B^+$ ,  $B^0$ ,  $B_s^0$  that consist of u (or  $\bar{u}$ ), d (or  $\bar{d}$ ), and s (or  $\bar{s}$ ) quark respectively, in addition to the b (or  $\bar{b}$ ) quark. From many decay modes of each  $B$  meson, the specific channel decays to  $J/\psi$  and a strange meson is chosen for this analysis.

$$\begin{aligned}
B^+ &\rightarrow J/\psi + K^\pm \rightarrow \mu^+ + \mu^- + K^\pm \\
B^0 &\rightarrow J/\psi + K_0^*(892) \rightarrow \mu^+ + \mu^- + K^+ + \pi^- \\
B_s^0 &\rightarrow J/\psi + \phi \rightarrow \mu^+ + \mu^- + K^+ + K^-
\end{aligned} \tag{1}$$

As this analysis does not separate corresponding antiparticle,  $B^+$  and  $B^-$ ,  $B^0$  and  $\bar{B}^0$ ,  $B_s^0$  and  $\bar{B}_s^0$  are denoted by  $B^+$ ,  $B^0$ ,  $B_s^0$ . For the final cross section values, the combined results are divided by two to obtain an average.

The CMS detector has highly efficient muon detection system and the high-resolution silicon tracker which is crucial to reconstruct  $B$  meson decays. The muon detector system, consisting of Cathode Strip Chambers (CSC), Drift Tubes (DT) and Resistive Plate chambers (RPC), is dedicated to identify and track the muons. The silicon tracker is located in the 3.8 T magnetic field generated by the superconducting solenoid, and consists of 1440 silicon pixel and 15148 silicon strip detector modules with a typical momentum resolution of 1.5 % in  $p_T$  for nonisolated particles of  $1 < p_T < 10$  GeV/c and  $|\eta| < 1.4$ , where  $\eta$  is the pseudo-rapidity in the laboratory frame. The detailed description of the CMS detector elements are given in Ref. [2].

For the pPb run lead nuclei of 1.58 TeV per nucleon collide with protons of 4 TeV. The center of mass energy is  $\sqrt{s_{NN}} = 5.02$  TeV. Because of the asymmetric beam energies, all produced particles from the collisions are detected with rapidity shift of 0.465 towards the proton-going side in the laboratory frame. The data sample used in this analysis corresponds to an integrated recorded luminosity of  $(34.6 \pm 1.2)$  nb $^{-1}$ .

## 2 Analysis

The events used in this analysis are collected with a single-muon trigger that requires at least one muon with  $p_T > 3$  GeV/c. The electromagnetic and beam-gas collision events are triggered by methods described in Ref.[3] The  $B$  reconstruction starts with the muons that are reconstructed from the inner tracker system and the outer muon system. The muons must satisfy the muon selection criteria including the kinematic limits imposed by the geometry of the detectors:  $p_T > 3.3$  GeV/c for  $|\eta| < 1.3$ ,  $p > 2.9$  GeV/c for  $1.3 < |\eta| < 2.2$  and  $p_T > 0.8$  GeV/c for  $2.2 < |\eta| < 2.4$ . The opposite-signed muon pairs used for this analysis are within  $\pm 300$  MeV/c $^2$  from its nominal  $J/\psi$  mass found in the Particle Data Group[4]. The charged hadrons are reconstructed by the inner tracker system within  $|\eta| < 2.4$  in the laboratory frame. To reconstruct  $B^+$ , the kaon mass is assigned to each charged particle and, then, the invariant-mass distribution of  $J/\psi$  plus kaon candidates are produced. The  $B^0$  and  $B_s^0$  analyses are more complicated than the charged  $B$ 's as they decay into the intermediate states which can be reconstructed by the two charged hadrons. Therefore, for the reconstructions of  $B^0$  and  $B_s^0$ , the pion and kaon masses are assigned to any pair of the charged particles.

In order to maximize the statistical significance of the  $B$  meson signals, selection is optimized for each meson species using a multivariate technique. The  $\chi^2$  of the secondary vertex fit, the distance between the primary and the secondary vertices (normalized by its uncertainty) and the cosine of the angle between the momentum vector of  $B$  and the position vector of the secondary vertex measured from the primary vertex in the transverse plane, etc. For the  $B^0$  and  $B_s^0$  reconstructions, additional constraints on the respective proper mass window of the invariant mass for the intermediate meson states are re-imposed. In the case of multiple  $B$  mesons being reconstructed in one event, the candidate with the best  $\chi^2$  of the secondary vertex is chosen to prevent the possible double counting.(especially, for the  $B^0$  case.)

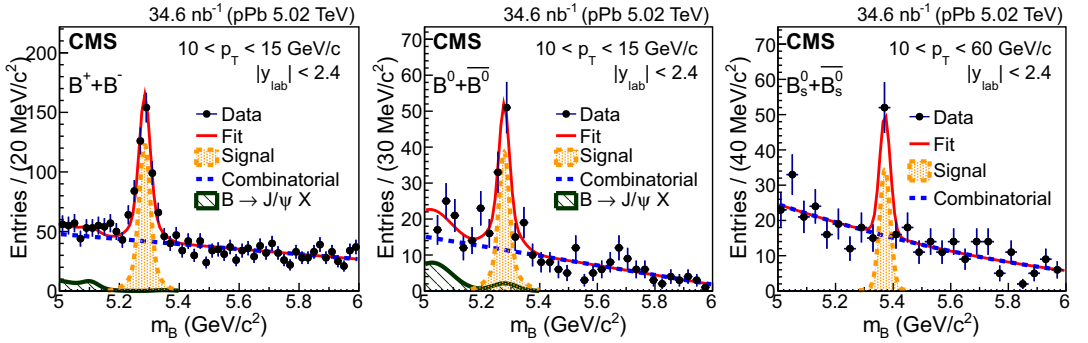


**Figure 1.** Invariant-mass distributions of  $B^+ + B^-$  (left),  $B^0 + \bar{B}^0$  (center), and  $B_s^0 + \bar{B}_s^0$  (right) candidates in the transverse momentum ranges of 10-15, 10-15 and 10-60 GeV/c respectively. The orange-dotted area represent the fitted  $B$  signal distributions and the green-hatched areas represent the peaking backgrounds from other  $B$  meson species. The blue-dotted lines represent the combinatorial backgrounds.

### 3 Results

All  $B$  candidates are reconstructed in  $10 < p_T < 60$  GeV/c and  $|y_{CM}| < 1.93$  where  $y_{CM}$  is the rapidity in center-of-mass frame. Fig. 1 shows the invariant-mass distribution of  $B^+$ ,  $B^0$  and  $B_s^0$  in their respective lowest  $p_T$  bin. The raw yields of  $B^+$ ,  $B^0$  and  $B_s^0$  are extracted using a binned maximum likelihood fit to the  $B$  meson invariant-mass distributions in the mass range  $5 < m_B < 6$  GeV/c<sup>2</sup>. The combinatorial backgrounds, fitted by first or second order polynomial functions, are dominated by inclusive  $J/\psi$ 's and charged hadrons associated with different mother particles. The so-called peaking background, shown by the green hatched areas in Fig. 1, is caused by the mis-reconstructed  $B$  mesons. In order to understand the signal and background distribution, Monte Carlo simulations have been performed. The particles in the Monte Carlo samples are generated by the PYTHIA event generator [5] and decayed by the EvtGen particle decay simulation package [6]. The initial and final state radiations are controlled by the PHOTOS package [7]. Furthermore, the signal particles are embedded in the HIJING minimum-bias events for pPb collisions to mimic more realistic environment [8]. After the proper background subtraction, several functions are tried to fit the signal peak shapes for each channel. Finally, sum of two Gaussian functions with same mean is chosen as the signal function.

The differential cross section for each  $B$  species has been obtained by

$$\left. \frac{d\sigma^B}{dp_T} \right|_{|y_{CM}| < 1.93} = \frac{1}{2} \frac{1}{\Delta p_T} \frac{N^B|_{|y_{CM}| < 1.93}}{(\alpha \times \epsilon) \cdot BR \cdot \mathcal{L}} \quad (2)$$

where  $\sigma^B$  is cross-section of  $B$ ,  $\Delta p_T$  is the width of the  $p_T$  bin,  $N^B$  is number of  $B$ ,  $\alpha$  is the geometrical acceptance,  $\epsilon$  is the efficiency estimated by the Monte Carlo simulation,  $BR$  is the branching ratio of the decay mode, and  $\mathcal{L}$  is the integrated luminosity. Note that the additional factor 1/2 is multiplied to take into account the charge conjugate of each  $B$  meson species such as  $B^-$  for  $B^+$ . For this analysis, the Fixed Order plus Next-to-Leading Logarithm (FONLL) calculations [9, 10] are used as the pp reference because the experimental pp data are not available at 5.02 TeV in the 2013 dataset. Note that FONLL has successfully reproduced the CDF data at 1.96 TeV and the CMS/ATLAS data at 7 TeV within the experimental and theoretical uncertainties [11, 12]. Using the analyzed differential

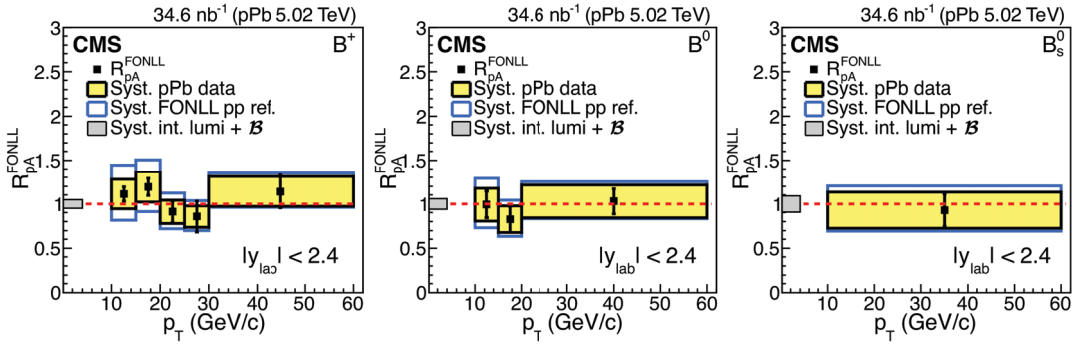


**Figure 2.** The nuclear modification factors  $R_{pA}^{\text{FONLL}}(p_T)$  of  $B^+$  (left),  $B^0$  (center),  $B_s^0$  (right) measured in pPb collisions at  $\sqrt{s_{NN}} = 5.02$  TeV. The statistical and systematic uncertainties on the pPb data are shown as bars and yellow boxes around the data points respectively. The systematic uncertainties from the FONLL predictions are plotted separately as open blue boxes. The global systematic uncertainties are shown as full grey boxes at unity, and are not included in the data points.

cross section data and the FONLL calculations, the nuclear modification factors are calculated by

$$R_{pA}^{\text{FONLL}}(p_T) = \frac{(d\sigma/dp_T)_{p\text{Pb}}}{A \times (d\sigma/dp_T)_{pp}} \quad (3)$$

where  $A$  is the number of nucleons in Pb. The results on  $R_{pA}^{\text{FONLL}}$  for  $B^+$ ,  $B^0$  and  $B_s^0$  are shown in Fig. 2. Within the systematic and statistical uncertainties,  $R_{pA}^{\text{FONLL}}$  of all three particle species are consistent with unity and, thus, significant cold nuclear matter effects are not observed. The nuclear modification factor as a function of rapidity in the center-of-mass frame is calculated only for the  $B^+$  which has the best statistical precision among the three analyzed particle species. In the Fig. 3 the left panel is differential cross section and right panel is nuclear modification factor of the  $B^+$ . Although the most backward data point toward the Pb-going side is higher than the others, the experimental uncertainties are large and no rapidity dependence can be claimed.

## 4 Conclusions

For the first time, the  $B^+$ ,  $B^0$ , and  $B_s^0$  mesons are exclusively reconstructed for  $10 < p_T < 60$  GeV/c and  $|y_{CM}| < 1.93$  in pPb collisions at  $\sqrt{s_{NN}} = 5.02$  TeV by the CMS Collaboration at the LHC. The range of transverse momentum covered is 10 to 60 GeV/c, for the rapidity range (evaluated in the center-of-mass frame) of  $|y_{CM}| < 1.93$ . Statistically significant peaks are observed for all three  $B$ -meson species in the invariant-mass distributions. The nuclear modification factors for all three  $B$ -meson species are estimated using FONLL calculations as pp references. The nuclear modification factors are consistent with unity within the uncertainties. Presently, the CMS Collaboration is analyzing the data recorded in 2015 with the 5.02 TeV PbPb collision. The present results will be baseline for the  $B$ -meson  $R_{AA}$ .

## References

[1] CMS Collaboration, J. High Energy Phys. 05 (2012) 063.

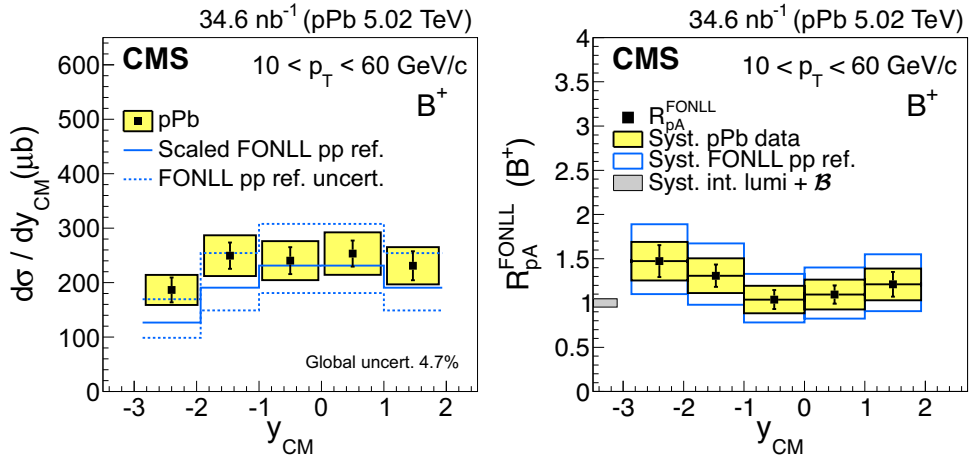


**Figure 3.** (left) The  $y_{CM}$ -differential production cross section of  $B^+$  measured in pPb collisions at  $\sqrt{s_{NN}} = 5.02$  TeV. Vertical bars (the boxes) correspond to statistical (systematic) uncertainties. The listed global systematic uncertainty is not included in the data points. The result is not included in the data points. The result is compared to a FONLL calculation represented by a continuous histogram. The dashed histograms represent the theoretical uncertainties for the FONLL reference. (right) The nuclear modification factor  $R_{pA}^{\text{FONLL}}(y_{CM})$  of  $B^+$  as a function of  $y_{CM}$ . The statistical and systematic uncertainties on the pPb data are shown as bars and yellow boxes around the data points, respectively. The systematic uncertainty from the FONLL reference is plotted separately as open blue boxes. The global systematic uncertainty is shown as a full grey box at unity, and is not included in the data points.

[2] CMS Collaboration, J Instruments. 3 (2008) S08004.  
 [3] CMS Collaboration, Eur. Phys. J. C 74 (2014) 2951.  
 [4] Particle Data Group Collaboration, Phys. Rev. D 86 (2012) 010001.  
 [5] T. Sjöstrand, S. Mrenna, P. Skands, J. High Energy Phys. 05 (2006) 026.  
 [6] D.J. Lange, Nucl. Instrum. Methods Phys. Res., Sect. A, Accel. Spectrom. Detect. Assoc. Equip. 462 (2001) 152.  
 [7] E. Barberio, B. van Eijk, Z. Was, Comput. Phys. Commun. 66 (1991) 115.  
 [8] X.-N. Wang, M. Gyulassy, Phys. Rev. D 44 (1991) 3501.  
 [9] M. Cacciari, S. Frixione, P. Nason, J. High Energy Phys. 0103 (2001) 006.  
 [10] M. Cacciari, M. Greco, P. Nason, J. High Energy Phys. 9805 (1998) 007.  
 [11] CDF Collaboration, Phys. Rev. D 75 (2007) 012010.  
 [12] ATLAS Collaboration, J. High Energy Phys. 10 (2013) 042.